arXiv:1604.00829v1 [nucl-th] 4 Apr 2016

# APPLICATION OF THE TRIAXIAL QUADRUPOLE-OCTUPOLE ROTOR TO THE GROUND AND NEGATIVE-PARITY LEVELS OF ACTINIDE NUCLEI

**M. S. Nadirbekov[1,3], N. Minkov[2], M. Strecker[3] and W. Scheid[3]**

[1] *Institute of Nuclear Physics, Ulughbek, Tashkent, 100214, Uzbekistan*
[2] *Institute of Nuclear Research and Nuclear Energy, 72 Tzarigrad Road, BG-1784 Sofia, Bulgaria*
[3] *Institut für Theoretische Physik der Justus-Liebig-Universität, Heinrich-Buff-Ring 16, D-35392 Giessen, Germany*

**Abstract:** In this work we examine the possibility to describe yrast positive- and negative-parity excitations of deformed even-even nuclei through a collective rotation model in which the nuclear surface is characterized by triaxial quadrupole and octupole deformations. The nuclear moments of inertia are expressed as sums of quadrupole and octupole parts. By assuming an adiabatic separation of rotation and vibration degrees of freedom we suppose that the structure of the positive- and negative- parity bands may be determined by the triaxial-rigid-rotor motion of the nucleus. By diagonalizing the Hamiltonian in a symmetrized rotor basis with embedded parity we obtain a model description for the yrast positive- and negative-parity bands in several actinide nuclei. We show that the energy displacement between the opposite-parity sequences can be explained as the result of the quadrupole-octupole triaxiality.

**Keywords:** Quadrupole and octupole deformations; alternating-parity spectra; triaxial rotor, staggering effect.

PACS Number(s): 21.10.Re, 21.60.Ev

## 1. Introduction

A basic problem in the collective excited states of even-even nuclei is the connection between the rotational motion and surface deformations with different multipolarities [1]. It is considered that the even-multipolarity deformations give rise to positive-parity states, while the odd-multipolarities can lead to the appearance of negative-parity states. Also, it is considered that the axial deformations play the leading role in the nuclear rotation collectivity, whereas the non-axial ones may be responsible for some specific properties of the spectra. Collective excited states with positive and/or negative parities in the cases of axial and non-axial deformations are explained by the early models [2]–[12]. In [4] an adiabatic approximation (separation of rotation motion from vibrations) was applied, providing

a possibility for description of positive-parity spectra of even-even nuclei for which the presence of non-axial quadrupole deformation is assumed. Also, some specific properties of rotational bands can be associated with the presence of effective quadrupole and octupole non-axial deformations. Based on such an assumption, the model approaches [6]-[9] attempt the simultaneous description of both, positive and negative-parity states, in even-even nuclei. From another side, it is commonly accepted that the appearance of negative-parity states is mainly determined by the octupole (reflection-asymmetric) deformations with the main contribution of the axial deformation mode [1, 13]. The spectroscopic properties of nuclei with assumed axial quadrupole and octupole deformations are considered in detail in [14]–[28] for different types of the potential energy depending on the surface deformation.

In this work a collective rotation model with non-axial quadrupole and octupole deformations is considered under the adiabatic approximation. It is applied for the simultaneous description of the ground-state (g.s.) and the lowest negative-parity bands of the even-even nuclei $^{228-232}$Th, $^{230-238}$U and $^{240}$Pu. In Refs. [6, 7, 8, 9] the non-axial deformations are treated similarly to the model of Davydov-Chaban [5], but without the use of the adiabatic approximation. In the present work the advantages of the adiabatic approximation are used to formulate a simplified pure rotor problem with respect to the nuclear surface parametrization explored in [9]. As a result the g.s. (positive-parity) and negative-parity levels of deformed even-even nuclei are considered as the excitations of a triaxial quadrupole-octupole rotor. In this approach the energy shift between the opposite-parity states is obtained as the result of the $K$-mixing effect due to the presence of quadrupole and octupole non-axial deformations. Based on the earlier interpretation [9] of the positive- and negative-parity excitations, the present approach is essentially different from the concept of pure octupole, or mixed quadrupole-octupole, vibrations and rotations. The latter concept assumes nuclear vibrations with respect to an octupole double-well [14]–[17], [24], or more general two-dimensional quadrupole-octupole potential with axial symmetry [18]–[23], [25]–[28] and rotations, used to explain the so-called alternating-parity spectra.

The purpose of this work is to quantitatively examine the possibility to explain the structure of alternating-parity bands within the triaxial quadrupole-octupole rotor concept based on the nowadays experimental data [29] on positive- and negative-parity energy levels in heavy even-even nuclei. As it will be seen below, the result can be compared to descriptions obtained within the quadrupole-octupole vibration-rotation concept. We think that such an investigation would provide a useful framework to evaluate the separate roles of the axial and non-axial degrees of freedom in the forming of collective spectra in the nuclei with quadrupole and octupole deformations as well as to examine the possibility to combine them into a common model approach.

In sec. 2 the quadrupole–octupole parametrization of the nuclear surface is briefly recalled. In sec. 3 the triaxial quadrupole–octupole rotor Hamiltonian and the solution of the eigenvalue problem for the alternating-parity excitations are presented. In sec. 4 results of the numerical application of the model to several even-even actinide nuclei are presented together with a relevant analysis and discussion of the model dynamic mechanism. In sec. 5 concluding remarks are given.

## 2. Quadrupole–octupole parametrization of the nuclear surface

The distance between the center of the deformed nucleus and its surface in the direction of the polar angles $\theta$, $\varphi$ in the laboratory frame $x$, $y$, $z$ is given by the expression [1, 3, 10, 11, 4]:

$$R(\theta,\varphi) = R_0\left[1+\sum_{\lambda\mu}\alpha_{\lambda\mu}Y^*_{\lambda\mu}(\theta,\varphi)\right], \tag{1}$$

where $R_0$ is the radius of the spherical shape. The parameters of nuclear deformations $\alpha_{\lambda\mu}$ satisfy the condition $\alpha^*_{\lambda\mu} = (-1)^\mu\alpha_{\lambda,-\mu}$, and for the spherical harmonics one has $Y^*_{\lambda\mu}(\theta,\varphi) = (-1)^\mu Y_{\lambda,-\mu}(\theta,\varphi)$. In the case of quadrupole and octupole deformations expression (1) can be written as

$$R(\theta,\varphi) = R_0\left[1+\sum_{\mu=-2}^{2}\alpha_{2\mu}Y^*_{2\mu}(\theta,\varphi)+\sum_{m=-3}^{3}\alpha_{3m}Y^*_{3m}(\theta,\varphi)\right]. \tag{2}$$

We introduce an intrinsic coordinate system the origin of which is fixed at the center of mass, with the axes $\xi$, $\eta$, $\zeta$ being directed along the principal axes of inertia of the nucleus. The orientation of the intrinsic axes with respect to the axes $x$, $y$, $z$ is defined by the Euler angles $\theta = \{\theta_1,\theta_2,\theta_3\}$, such that

$$R(\theta',\varphi') = R_0\left[1+\sum_{\nu=-2}^{2}a_{2\nu}Y^*_{2\nu}(\theta',\varphi')+\sum_{m=-3}^{3}a_{3m}Y^*_{3m}(\theta',\varphi')\right], \tag{3}$$

with

$$a_{\lambda\nu} = \sum_\mu \alpha_{\lambda\mu}D^{*\lambda}_{\nu\mu}(\theta), \qquad \alpha_{\lambda\mu} = \sum_\nu D^\lambda_{\mu\nu}(\theta)a_{\lambda\nu}, \qquad \lambda = 2,3,$$

where $D^\lambda_{\mu\nu}(\theta)$ is the Wigner function according to [30].

A possible parametrization [3, 7] of the quadrupole-octupole shape in the intrinsic coordinate system is

$$a_{2,1} = a_{2,-1} = 0, \qquad a_{3,\pm1} = a_{3,\pm3} = 0 \tag{4}$$

and

$$a_{2,0} = \beta_2\cos\gamma, \qquad a_{2,2} = a_{2,-2} = \frac{\beta_2\sin\gamma}{\sqrt{2}}, \tag{5}$$

$$a_{3,0} = \beta_3\cos\eta, \qquad a_{3,2} = a_{3,-2} = \frac{\beta_3\sin\eta}{\sqrt{2}}, \tag{6}$$

where $\beta_2 \geq 0$ and $\gamma$ ($0 \leq \gamma \leq \frac{\pi}{3}$ in the case of pure quadrupole deformation) are the parameters of axial and triaxial quadrupole deformations, respectively [3]; $\beta_3$ and $\eta$ ($0 \leq \eta \leq \frac{\pi}{2}$ in the case of pure octupole deformation) are the parameters of axial and triaxial octupole deformations, respectively [7]. We remark that the case $a_{3,\pm1} \neq 0, a_{3,\pm3} \neq 0$ was considered in [8], whereas in [31] it was shown that deformation degrees of freedom determined by $a_{3,\pm3}$ can be associated with pure two-quasiparticle states and may not need to be considered as collective variables. Also, in the above parametrization (4)-(6) the octupole shape is aligned with respect to the quadrupole ellipsoid which determines the body-fixed frame.

## 3. Triaxial quadrupole-octupole rotor in adiabatic approximation

After imposing the adiabatic approximation the collective rotation motion of the nucleus is considered separately from the other degrees of freedom. If no further assumptions (e.g. axial symmetry) are imposed, the corresponding energy spectrum is described by the triaxial-rotor Hamiltonian

$$\hat{H}_{\rm rot} = \sum_{i=1}^{3} \frac{\hbar^2 \hat{I}_i^2}{2\mathfrak{J}_i}, \tag{7}$$

where $\hat{I}_i$ $(i = 1, 2, 3)$ are the components of the angular momentum operator and $\mathfrak{J}_i$ are the respective components of the moment of inertia. By applying the parametrization (4)-(6) into the expansion (3) the latter are obtained in a form corresponding to a triaxial quadrupole-octupole shape [9]

$$\mathfrak{J}_1 = 8B_2\beta_2^2 \sin^2\left(\gamma - \frac{2\pi}{3}\right) + 8B_3\beta_3^2 \left[\frac{3}{2}\cos^2\eta + \sin^2\eta + \frac{\sqrt{15}}{2}\sin\eta\cos\eta\right] \tag{8}$$

$$\mathfrak{J}_2 = 8B_2\beta_2^2 \sin^2\left(\gamma - \frac{4\pi}{3}\right) + 8B_3\beta_3^2 \left[\frac{3}{2}\cos^2\eta + \sin^2\eta - \frac{\sqrt{15}}{2}\sin\eta\cos\eta\right] \tag{9}$$

$$\mathfrak{J}_3 = 8B_2\beta_2^2 \sin^2\gamma + 8B_3\beta_3^2 \sin^2\eta, \tag{10}$$

where $\mathfrak{J}_i$ $(i = 1, 2, 3)$ explicitly depend on the quadrupole and octupole mass and deformation parameters $B_2$, $\beta_2$, $\gamma$ and $B_3$, $\beta_3$, $\eta$, respectively.

In the present work we consider (under the assumption of the adiabatic approximation) the deformation parameters (or more precisely their average values) as constants whose values $\beta_{2\,\rm eff}$, $\gamma_{\rm eff}$ and $\beta_{3\,\rm eff}$, $\eta_{\rm eff}$, effectively determine a rigid triaxial rotor. Since the mass parameters and the squares of the axial deformation parameters enter the moments of inertia components as *products* we introduce in (8)–(10) the following parameters $\tilde{B}_2{=}8B_2\beta_{2\,\rm eff}^2$ and $\tilde{B}_3{=}8B_3\beta_{3\,\rm eff}^2$. Thus we obtain the quadrupole-octupole moment of inertia in a form depending on *four* arguments $\mathfrak{J}_i = \mathfrak{J}_i(\tilde{B}_2, \tilde{B}_3, \gamma_{\rm eff}, \eta_{\rm eff})$. We take these arguments, $\tilde{B}_2, \tilde{B}_3, \gamma_{\rm eff}, \eta_{\rm eff}$, as *adjustable parameters*. By introducing the reciprocal inertia factors $A_i(\tilde{B}_2, \tilde{B}_3, \gamma_{\rm eff}, \eta_{\rm eff}) = 1/[2\mathfrak{J}_i(\tilde{B}_2, \tilde{B}_3, \gamma_{\rm eff}, \eta_{\rm eff})]$ $(i = 1, 2, 3)$ we get the Hamiltonian (7) in the form

$$\hat{H}_{\rm rot} = \sum_{i=1}^{3} \hbar^2 A_i(\tilde{B}_2, \tilde{B}_3, \gamma_{\rm eff}, \eta_{\rm eff}) \hat{I}_i^2 \tag{11}$$

depending on the four parameters $\tilde{B}_2, \tilde{B}_3, \gamma_{\rm eff}, \eta_{\rm eff}$.

Here it is important to remark that the involvement of the quantities $\tilde{B}_2$ and $\tilde{B}_3$ assumes a more general dependence of the moment of inertia on the respective mass and axial-deformation parameters. In this way the solution of the rotation energy problem does not constrain the mass and deformation parameters separately but only determines their products. In the context of the more general rotation-vibration problem (not considered here) this means that $\tilde{B}_2$ and $\tilde{B}_3$ can be interpreted as generalized mass parameters

carrying implicit dependence (not necessarily quadratic) on the axial quadrupole and octupole deformations. From this aspect the situation resembles the concept of deformation-dependent-mass approaches where some plausible dependencies of the mass parameter on the axial quadrupole deformation are assumed under proper physical argumentation [32, 33, 34, 35, 36]. As here the vibration energy is not considered, the parameters $\tilde{B}_2$ and $\tilde{B}_3$ only determine the general scale of the rotation energy and the relative contributions of the quadrupole and octupole deformations in the moment of inertia, while their particular deformation dependence does not play a role.

The energy spectrum of the above determined triaxial quadrupole-octupole rotor is obtained by diagonalizing the Hamiltonian (7) in the basis of the symmetrized rotor functions with built-in parity [9]

$$|IMK\pm\rangle = \frac{1}{\sqrt{2(1+\delta_{K,0})}}\left(|IMK\rangle \pm (-1)^{I-K}|IM-K\rangle\right) \ , \tag{12}$$

where $|IMK\rangle = \sqrt{\frac{2I+1}{8\pi^2}}D^I_{MK}(\theta)$, and $M$ and $K$ are the projections of the angular momentum $\hat{I}$ on the third axes of the laboratory and intrinsic frames, respectively. The eigenfunctions are obtained in the form

$$\Phi^{\pm}_{IMn}(\theta) = \sum_{K\geq 0}^{I} C^n_{IK}|IMK\pm\rangle \ . \tag{13}$$

The expansion coefficients implicitly depend on the effective mass and deformation parameters: $C^n_{IK} = C^n_{IK}(\tilde{B}_2, \tilde{B}_3, \gamma_{\rm eff}, \eta_{\rm eff})$. For given angular momentum $I$ the quantum number $n = 0, 1, 2, \ldots$ (limited by $K \leq I$) labels the different eigenvalues $E^n(I)$ of $\hat{H}_{\rm rot}$ in ascending order.

We obtain the matrix elements of Hamiltonian (7) between basis states (12) with different $K$-values in the following general form

$$\begin{aligned}
&\langle IMK' \pm |\hat{H}_{\rm rot}|IMK\pm\rangle = \frac{1}{\sqrt{(1+\delta_{K',0})(1+\delta_{K,0})}} \\
\times\ &\left\{\frac{1}{2}\left[(A_1+A_2)I(I+1) - (A_1+A_2-2A_3)K^2\right]\left[\delta_{K'K} \pm (-1)^{I-K}\delta_{K',-K}\right]\right. \\
+\ &(A_1-A_2)f(I,K)\left[\delta_{K',K+2} \pm (-1)^{I-K}\delta_{K',-K-2}\right] \\
+\ &\left.(A_1-A_2)f(I,-K)\left[\delta_{K',K-2} \pm (-1)^{I-K}\delta_{K',-K+2}\right]\right\},
\end{aligned} \tag{14}$$

with

$$f(I,K) = \frac{1}{4}\sqrt{(I+K+2)(I+K+1)(I-K-1)(I-K)}. \tag{15}$$

Since $K, K' \geq 0$, in (14) one has $\delta_{K',-K} \neq 0$ only for $K = 0$, $\delta_{K',-K+2} \neq 0$ only for $K = 0, 1, 2$, while $\delta_{K',-K-2}$ is always zero. As a result Eq. (14) can be written in a bit

simpler form

$$\begin{aligned}
&\langle IMK' \pm |\hat{H}_{\rm rot}|IMK\pm\rangle = \frac{1}{2\sqrt{(1+\delta_{K',0})(1+\delta_{K,0})}} \\
\times\ &\left\{\left[(A_1+A_2)I(I+1)-(A_1+A_2-2A_3)K^2\right]\left[\delta_{K'K}\pm(-1)^{I-K}\delta_{K',-K}\right]\right. \\
+\ &\left. 2(A_1-A_2)\left[f(I,K)\delta_{K',K+2}+f(I,-K)\left(\delta_{K',K-2}\pm(-1)^{I-K}\delta_{K',-K+2}\right)\right]\right\}. \quad (16)
\end{aligned}$$

Here we make the following important assumptions originally imposed in [9]:

(i) The quantum number $K$ takes only even values (see also [6, 10, 12]). Then in (13) the sum over $K$ runs from 0 to $I$ in steps of 2.

(ii) The (+) and (−) phases in (13) and(12), which correspond to the $A$ and $B_1$ classes of the rotation group $D_2$, are attributed to the positive- and negative-parity states, respectively.

Because of (i) the phase factor $(-1)^K = 1$ can be omitted in the matrix element expressions (14) and (16). According to (ii) one can write $\Phi^{\pm}_{IMn} \equiv \Phi^{\pi}_{IMn}$ and $|IMK\pm\rangle \equiv |IMK\pi\rangle$ in (13) and (12), respectively, where $\pi = \pm$ is the parity of the rotation state. Also, according to (12) the $\pi = (+)$ parity corresponds to $I =$ even angular momentum states and $\pi = (-)$ corresponds to $I =$ odd, as in the usual alternating-parity (octupole) bands. Therefore, one has $\pi = (-1)^I$. Then the $(\pm)$ and phase factors in (14) and (16) can be omitted when alternating-parity bands are considered. As a result the matrix element (16) reads

$$\begin{aligned}
&\langle IMK'\pi|\hat{H}_{\rm rot}|IMK\pi\rangle = \frac{1}{2\sqrt{(1+\delta_{K',0})(1+\delta_{K,0})}} \\
\times\ &\left\{\left[(A_1+A_2)I(I+1)-(A_1+A_2-2A_3)K^2\right]\left[\delta_{K'K}+\delta_{K',-K}\right]\right. \\
+\ &\left. 2(A_1-A_2)\left[f(I,K)\delta_{K',K+2}+f(I,-K)\left(\delta_{K',K-2}+\delta_{K',-K+2}\right)\right]\right\}. \quad (17)
\end{aligned}$$

Note that the righthand side of (17) does not include $\pi$ explicitly, whereas as mentioned above, it is implied by the value of $I$ (even or odd). The lowest eigenvalues $E^{n=0}(I)$ and eigenfunctions $\Phi^{\pi}_{IM(n=0)}$ of the Hamiltonian correspond to the g.s. band for $I =$even, and to the lowest negative-parity band for $I =$odd. In the same way the higher eigenfunctions/eigenvalues with $n = 1, 2, ...$ determine higher sets of positive- and negative-parity bands. In this work we only consider the lowest (yrast) band structure with $n = 0$.

Now, one can easily check that due to the non-diagonal matrix elements in (17), which mix the basis states with $\Delta K = 2$, the negative-parity levels appear shifted up in energy with respect to the positive-parity levels in the g.s. band. The magnitude of the shift depends on the values of the non-diagonal matrix elements. It increases with the increase of the quadrupole and octupole non-axiality parameters $\gamma_{\rm eff}$ and $\eta_{\rm eff}$ and decreases with the increase of the angular momentum. In this way the considered triaxial quadrupole-octupole rotor approach allows a possibility to reproduce the observed behaviour of the lowest nuclear positive- and negative-parity bands, which are often interpreted as an yrast alternating-parity band.

In the present approach the staggering effect observed in the alternating-parity bands appears as the result of two model features: 1) association of the parity of the observed

rotation states (the +/- phases in (13) and (12)) with the parity of the angular momentum values, and 2) mixing of different K-modes due to the assumed triaxial deformations.

We remark that although the triaxial rotor Hamiltonian (7) mixes different K-modes it does not mix the parity. Therefore, the rotation states appearing in the model have a well-defined parity. It should be noted that also the intrinsic state which is presently adiabatically separated is usually considered with a good parity. Thus, when it is associated with a double-well potential one gets the lowest potential level whose (determined) parity combined with the parity of the rotation-mode provides a good parity of the total (observed) state. More details on that issue are given e.g. in ref. [24]. In the present approach, due to the adiabatic approximation, the intrinsic parity is directly built in the parity of the observed rotation state through the parity of the angular momentum value $(-1)^I$.

## 4. Numerical results and discussion

The theoretical spectrum obtained through the above diagonalization procedure was applied to *simultaneously* describe the yrast positive- and negative-parity levels of several actinide nuclei: $^{228,230,232}$Th, $^{230,232,234,236,238}$U and $^{240}$Pu and shown in Figs. 1-9. The triaxial quadrupole-octupole rotor parameters $\tilde{B}_2$, $\tilde{B}_3$, $\gamma_{\rm eff}$ and $\eta_{\rm eff}$ were adjusted to experimental data through a least-square fitting procedure. The theoretical and experimental energy values are compared in Figs. 1-9 (left). To get more detailed information about the angular momentum behaviour of the theoretical and experimental alternating-parity sequences we apply the following odd-even staggering formula [25]

$$Stg(I) = 6\Delta E(I) - 4\Delta E(I-1) - 4\Delta E(I+1) + \Delta E(I+2) + \Delta E(I-2), \qquad (18)$$

with $\Delta E(I) = E(I+1) - E(I)$. The obtained theoretical and experimental staggering patterns are presented in Figs. 1-9 (right). The adjusted parameter values and the root-mean-square (RMS) deviations between theoretical and experimental energy values are given in the captions.

Here, we can make the following comments.

In the nuclei $^{228}$Th (RMS=66.2 keV), $^{230}$U (RMS=70.3 keV), $^{232}$U (RMS=39.4 keV), $^{234}$U (RMS=11.3 keV) and $^{238}$U (RMS=68.3 keV) the model description is relatively good. The obtained RMS values are comparable with the values obtained in models where the alternating-parity bands are described as the result of mixed quadrupole-octupole vibrations and rotations [25, 27, 28]. We remark that in the nuclei $^{230,232,234,238}$U the staggering amplitude shows a slow decrease without reaching zero.

In the remaining nuclei, $^{230}$Th (RMS=119.3 keV), $^{232}$Th (RMS=160 keV), $^{236}$U (RMS= 145.5 keV) and $^{240}$Pu (RMS=132.4 keV) the deviation between theory and experiment is essentially larger with RMS>100 keV. This is also observed in the staggering diagrams in figures 2, 3, 7 and 9, where the experimental staggering amplitude decreases more rapidly compared to the theoretical one. It is clear that in these cases the $K$-mixing effect generated by the model triaxial rotations remains too strong in the high angular momentum $I$. As a result the energy shift between positive- and negative-parity sequences in the theoretical spectrum remains large, causing a more persistent staggering effect. Thus, the model reproduces with a less accuracy the fine structure of spectra where a single (less perturbed)

alternating-parity band is formed at high angular momentum. We remark that in three of the nuclei, $^{228,230}$Th and $^{240}$Pu, the experimental staggering reaches zero amplitude at high angular momentum and then reappears with a changed phase. This behaviour is known as a "beat" staggering effect, and corresponds to more complicated properties of the rotating quadrupole-octupole nucleus. It was explained, e.g. in the so-called quadrupole-octupole rotation model (QORM) [24], and remains beyond the present approach.

Also, we should remark that a more general source of discrepancy between theory and experiment in all nuclei under study is the fact that we consider a rigid rotor which is, of course, a rather robust assumption. We see that in the nuclei $^{230,232,234,238}$U, where the experimental spectrum is developed up to a not very high angular momentum, the model effect of rigidity is small, allowing an overall good description of the experimental bands.

To get more detailed insight into the physical contents of the results obtained we have to analyze the model parameters values. First we note that the effective mass contribution, $\tilde{B}_2 \sim 100\ \hbar^2 MeV^{-1}$, of the quadrupole deformation is by two orders of magnitude larger than the octupole one $\tilde{B}_3 \sim 1\ \hbar^2 MeV^{-1}$. This means that the quadrupole deformation enters the problem as a leading collective mode, whereas the octupole deformation is superposed as a small correction. We notice that $\tilde{B}_2$ and $\tilde{B}_3$ values used in the model are very narrow localized around $100\ \hbar^2 MeV^{-1}$ and $1\ \hbar^2 MeV^{-1}$, respectively, which means that the overall energy scale of the collective motion of the different nuclei considered in the model is quite uniquely determined.

Also, we see that the obtained values of the triaxiality parameters vary in quite narrow limits, with the quadrupole-triaxiality $\gamma_{\text{eff}}$ varying between 50° and 57°, and the octupole-triaxiality $\eta_{\text{eff}}$ varying between 48° and 50°.

The obtained results suggest:

i) in the considered nuclei the energy shift between even and odd angular momentum levels with positive and negative parity, respectively, can be generated by the simultaneous presence of quadrupole and octupole triaxial deformations. As such it might be associated with the $K$-mixing and not only with the parity effect.

ii) The $\gamma$-deformation approaching 60° corresponds to an overall oblate quadrupole shape, whereas the presence of the octupole-deformation components suggests a more complicated shape structure. Although the present model descriptions contradict the common understanding about pronounced axial deformations manifesting in the heavy actinide nuclei, this study shows that the triaxial rotor concept may serve as a basis for an extended consideration of nuclear quadrupole-octupole rotations and vibrations with the presence of non-axial degrees of freedom.

## 5. Conclusion

In this work we evaluated the capability of the triaxial quadrupole-octupole rotor to describe the structure of the lowest positive- and negative-parity levels in the spectra of heavy even-even nuclei. It is shown that by using two (quadrupole and octupole) mass parameters and two (quadrupole and octupole) triaxiality parameters, all of them varying in the considered nuclei in quite narrow limits. We are able to reproduce the overall structure of the lowest alternating-parity energy sequences in several actinide nuclei. Although the

result is comparable to the descriptions obtained within the quadrupole-octupole vibration-rotation concept, it corresponds to a different collective mechanism based on the $K$-mixing effect. The latter is due to the assumption of strong quadrupole and octupole triaxialities (with the quadrupole deformation being the leading mode) which according to the model are responsible for the energy shift between the positive- and negative-parity sequences. On this basis we conclude that the triaxial quadrupole-octupole rotor approach could provide a useful tool to evaluate and compare the contributions of the axial and non-axial quadrupole and octupole deformations in the collective motion of nuclei. Further more detailed investigation beyond the adiabatic approximation, including the related vibration modes, will be necessary to connect the different approaches to the problem of alternating-parity spectra in even-even nuclei.

## Acknowledgments

Dr. M. S. Nadirbekov thanks Prof. W. Scheid for the invitation under the DAAD program to the Institute for Theoretical Physics (Giessen, Germany). Financial supports from the Uzbekistan Academy of Sciences under contract No. F2-FA-F117 and by the Bulgarian National Science Fund under contract No. DFNI-E02/6 are gratefully acknowledged.

# References


[1] J. M. Eisenberg and W. Greiner, *Nuclear Theory: Nuclear Models* (North-Holland, Amsterdam, 1987), third, revised and enlarged edition, Vol. I.

[2] A. Bohr, *Dan. Mat. Fys. Medd.* **26**, No. 14 (1952)14.

[3] A. Bohr, B. R. Mottelson, *Dan. Mat. Fys. Medd.* **27**, No. 16 (1953).

[4] A. S. Davydov and G. F. Filippov, *Nucl. Phys.* **8** (1958) 237.

[5] A. S. Davydov and A. A. Chaban, *Nucl. Phys.* **20** (1960) 499.

[6] S. A. Williams and J. P. Davidson, *Can. J. Phys.* **40** (1962) 1423.

[7] J. P. Davidson, *Nucl. Phys.* **33** (1962) 664.

[8] M. G. Davidson, *Nucl. Phys.* **69** (1965) 455.

[9] M. G. Davidson, *Nucl. Phys. A* **103** (1967) 153.

[10] J. P. Davidson, *Rev. Mod. Phys.* **37** (1965) 105.

[11] J. P. Davidson, *Collective Models of the Nucleus* (Academic Press Inc., New York, 1968).

[12] A. S. Davydov, *Excited States of Atomic Nuclei* (Atomizdat, Moscow,1967) (in Russian).

[13] P. A. Butler and W. Nazarewicz, *Rev. Mod. Phys.* **68** (1996) 349.

[14] H. J. Krappe and U. Wille, *Nucl. Phys. A* **124**, 641 (1969).

[15] G. A. Leander, R. K. Sheline, P. Möller, P. Olanders, I. Ragnarsson, and A. J. Sierk, *Nucl. Phys. A* **388** (1982) 452.

[16] R. V. Jolos, P. von Brentano, and F. Dönau, *J. Phys. G: Nucl. Part. Phys.* **19** (1993) L151.

[17] R. V. Jolos, P. von Brentano, *Phys. Rev. C* **49** (1994), R2301.

[18] V. Yu. Denisov, *Sov. J. Nucl. Phys* **49** (1989) 399.

[19] A. Ya. Dzuyblik and V. Yu. Denisov, *Ukr. Phys. J.* **37** (1992) 1770.

[20] A. Ya. Dzuyblik and V. Yu. Denisov, *Phys. At. Nucl.* **56** (1993) 303.

[21] V. Yu. Denisov and A. Ya. Dzuyblik, *Phys. At. Nucl.* **56** (1993) 477.

[22] V. Yu. Denisov and A. Ya. Dzyublik, *Nucl. Phys. A* **589** (1995) 17.

[23] Sh. Sharipov and M. S. Nadirbekov, *Ukr. Phys. J.* **50** (2005) 21.

[24] N. Minkov, P. Yotov, S. Drenska and W. Scheid, *J. Phys. G: Nucl. Part. Phys.* **32** (2006) 497.

[25] N. Minkov, P. Yotov, S. Drenska, W. Scheid, D. Bonatsos, D. Lenis and D. Petrellis, *Phys. Rev. C* **73** (2006) 044315.

[26] N. Minkov, S. Drenska, P. Yotov *et al., Phys. Rev. C* **76** (2007) 034324.

[27] N. Minkov, S. Drenska, M. Strecker, W. Scheid and H. Lenske, *Phys. Rev. C* **85** (2012) 034306.

[28] M. S. Nadirbekov, G. A. Yuldasheva, N. Minkov and W. Scheid, *Int. J. Mod. Phys. E* **21** (2012) 1250044.

[29] http://www.nndc.bnl.gov/ensdf/, Evaluated and Compiled Nuclear Structure Data: ENSDF and XUNDL Dataset Retrieval.

[30] A. R. Edmonds, *Angular Momentum in Quantum Mechanics* (Princeton University Press, Princeton, 1957).

[31] V. G. Soloviev, P. Vogel and A. A. Korneichuk, *Izv. Akad. Nauk. SSSR. (Ser. Fiz.)* **28** (1964) 1512.

[32] R. V. Jolos, P. von Brentano, *Phys. Rev. C* **78** (2008) 064309.

[33] R. V. Jolos, P. von Brentano, *Phys. Rev. C* **79** (2009) 044310.

[34] D. Bonatsos, P. Georgoudis, D. Lenis, N. Minkov and C. Quesne, *Phys. Lett. B* **683** (2010), 264-271.

[35] D. Bonatsos, P. Georgoudis, D. Lenis, N. Minkov and C. Quesne, *Phys. Rev. C* **83** (2011) 044321.

[36] D. Bonatsos, P. E. Georgoudis, N. Minkov, D. Petrellis and C. Quesne, *Phys. Rev. C* **88** (2013) 034316.

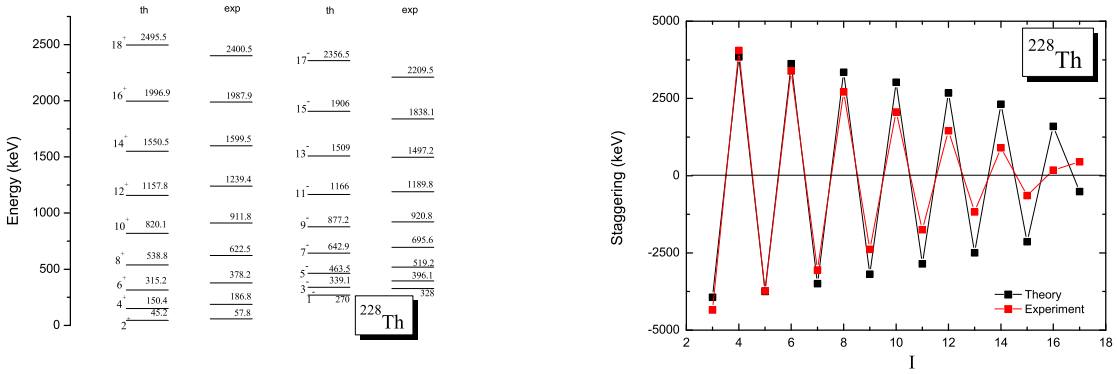


Figure 1: Theoretical and experimental energy levels (left) and odd-even staggering patterns (right) for the nucleus $^{228}$Th (parameters values: $\tilde{B}_2$=90.2$\hbar^2 MeV^{-1}$, $\tilde{B}_3$=1$\hbar^2 MeV^{-1}$, $\gamma_{\rm eff}$=52.2586°, $\eta_{\rm eff}$=48.3071° and RMS=66.2 keV).

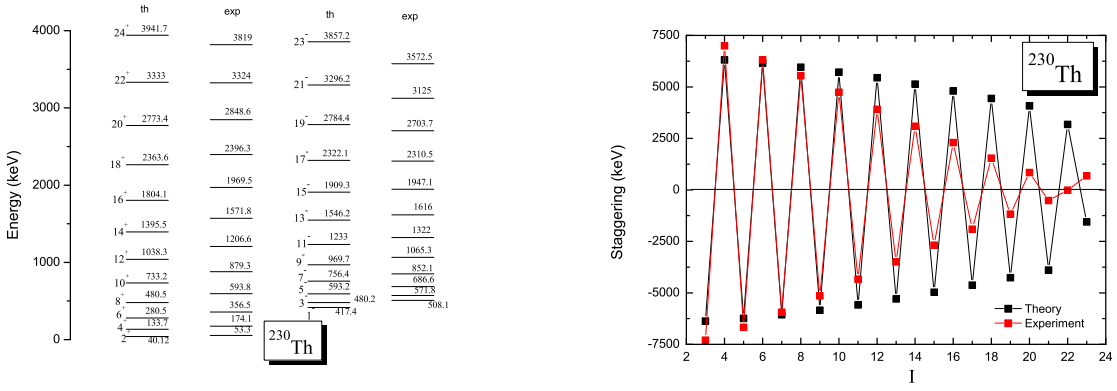


Figure 2: The same as in Fig.1, but for $^{230}$Th (parameters values: $\tilde{B}_2$=100$\hbar^2 MeV^{-1}$, $\tilde{B}_3$=1$\hbar^2 MeV^{-1}$, $\gamma_{\rm eff}$=54.3776°, $\eta_{\rm eff}$=49.3124° and RMS=119.3 keV).

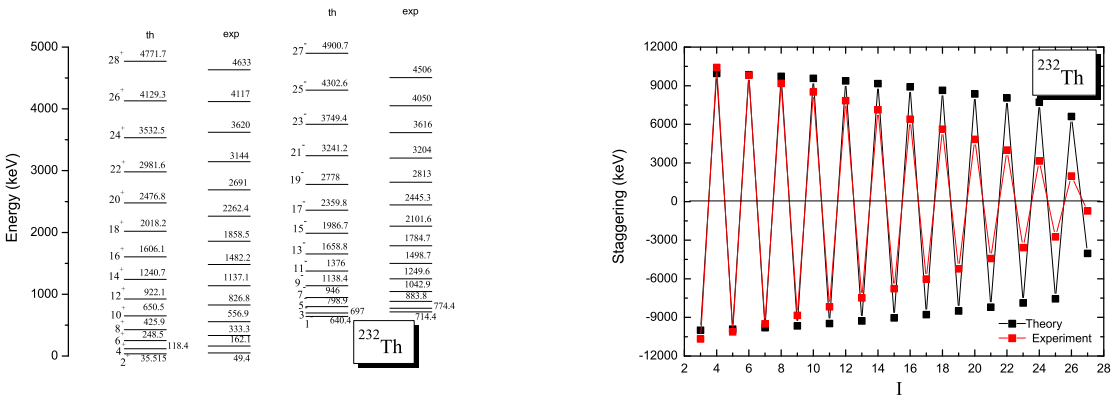


Figure 3: The same as in Fig.1, but for $^{232}$Th (parameters values: $\tilde{B}_2$=112$\hbar^2 MeV^{-1}$, $\tilde{B}_3$=1.011$\hbar^2 MeV^{-1}$, $\gamma_{\rm eff}$=56.0482°, $\eta_{\rm eff}$=50.1441° and RMS=160 keV).

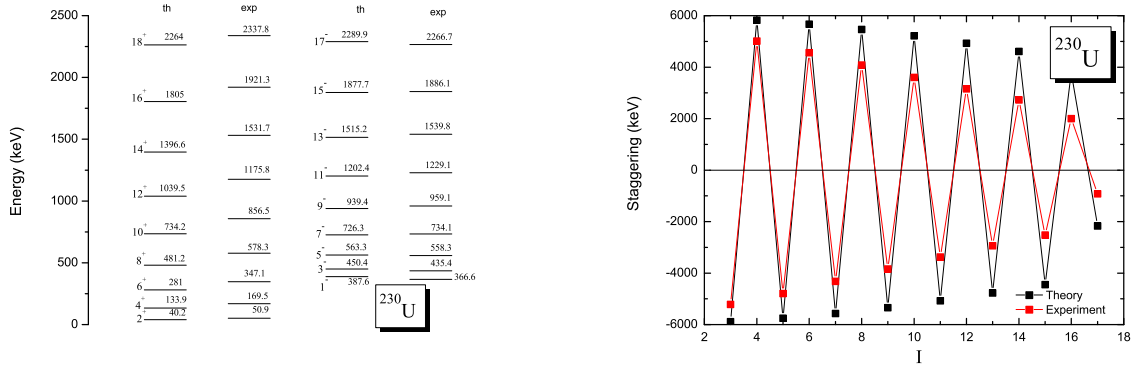


Figure 4: The same as in Fig.1, but for $^{230}$U (parameters values: $\tilde{B}_2$=100$\hbar^2 MeV^{-1}$, $\tilde{B}_3$=1$\hbar^2 MeV^{-1}$, $\gamma_{\rm eff}$=54.1076°, $\eta_{\rm eff}$=49.1587° and RMS=70.3 keV).

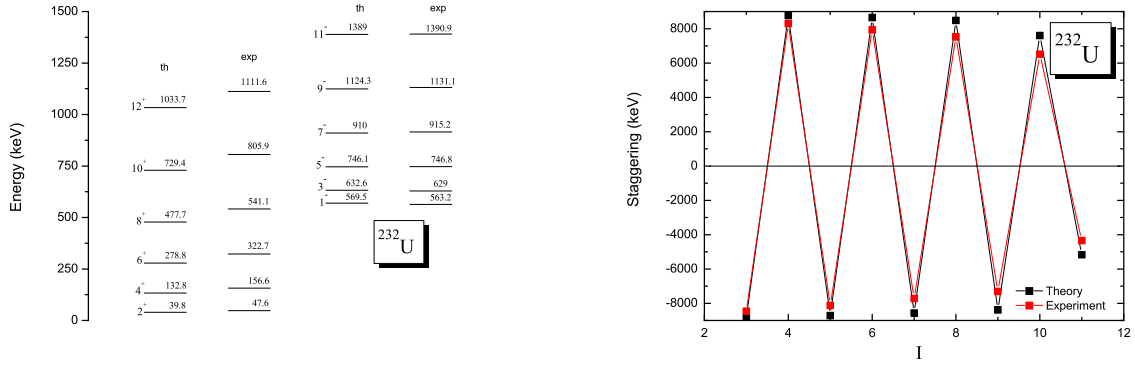


Figure 5: The same as in Fig.1, but for $^{232}$U (parameters values: $\tilde{B}_2$=100$\hbar^2 MeV^{-1}$, $\tilde{B}_3$=1$\hbar^2 MeV^{-1}$, $\gamma_{\rm eff}$=55.4337°, $\eta_{\rm eff}$=49.8625° and RMS=39.4 keV).

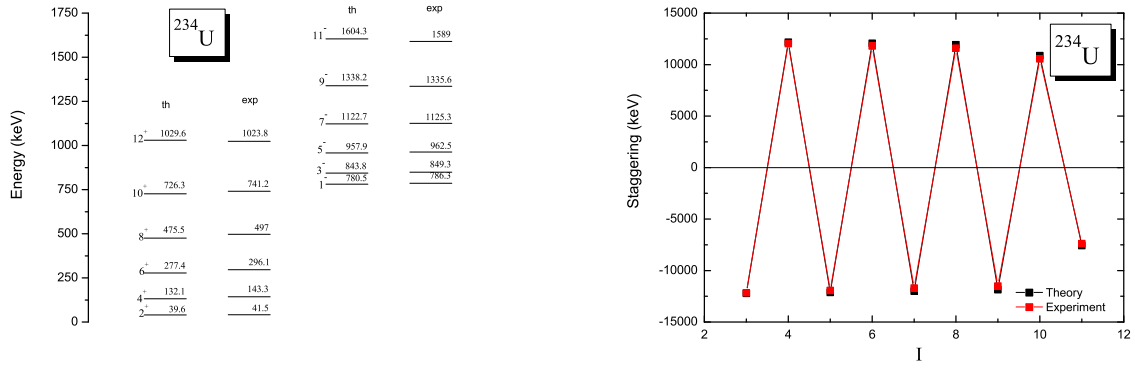


Figure 6: The same as in Fig.1, but for $^{234}$U (parameters values: $\tilde{B}_2$=100$\hbar^2 MeV^{-1}$, $\tilde{B}_3$=1$\hbar^2 MeV^{-1}$, $\gamma_{\rm eff}$=56.4036°, $\eta_{\rm eff}$=50.3398° and RMS=11.3 keV).

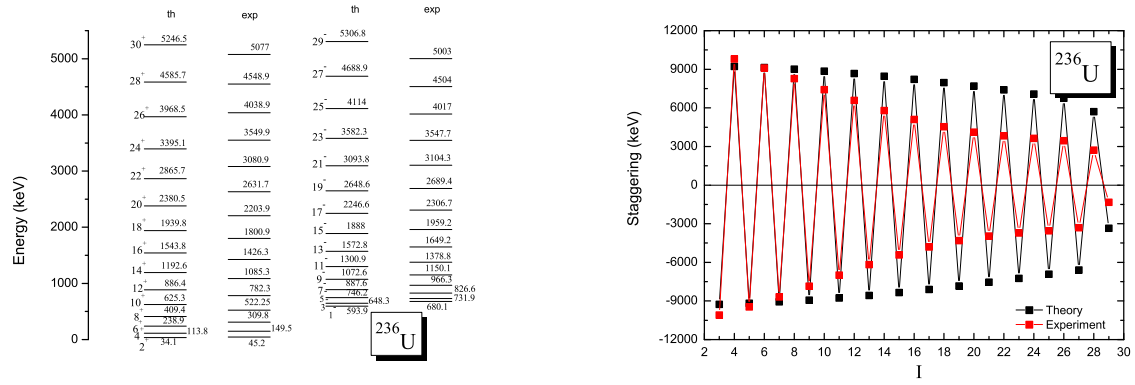


Figure 7: The same as in Fig.1, but for $^{236}$U (parameters values: $\tilde{B}_2$=116.1$\hbar^2 MeV^{-1}$, $\tilde{B}_3$=1.268$\hbar^2 MeV^{-1}$, $\gamma_{\rm eff}$=56.1288°, $\eta_{\rm eff}$=50.1802° and RMS=145.5 keV).

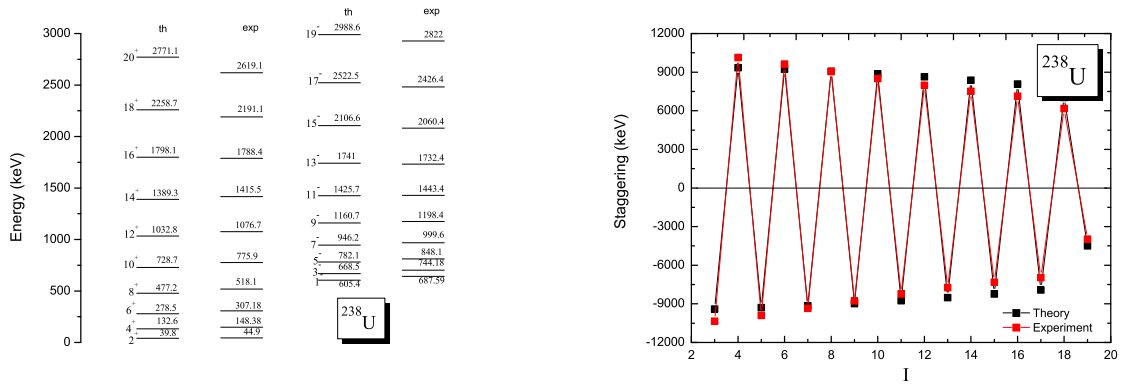


Figure 8: The same as in Fig.1, but for $^{238}$U (parameters values: $\tilde{B}_2$=100$\hbar^2 MeV^{-1}$, $\tilde{B}_3$=1$\hbar^2 MeV^{-1}$, $\gamma_{\rm eff}$=55.6287°, $\eta_{\rm eff}$=49.9292° and RMS=69.3 keV).

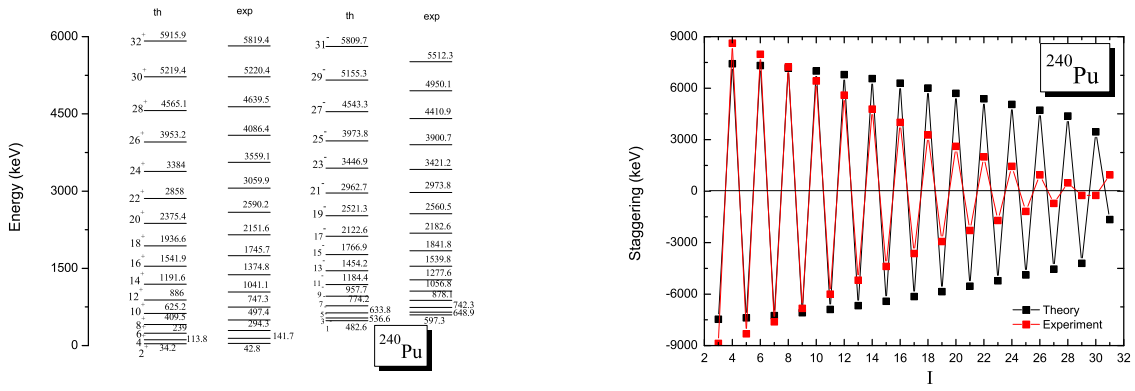


Figure 9: The same as in Fig.1, but for $^{240}$Pu (parameters values: $\tilde{B}_2$=117$\hbar^2 MeV^{-1}$, $\tilde{B}_3$=1.02$\hbar^2 MeV^{-1}$, $\gamma_{\rm eff}$=55.2914°, $\eta_{\rm eff}$=49.7773° and RMS=132.4 keV).